*Article*

# Improving Transient Stability of a Synchronous Generator Using UIPC with a Unified Control Scheme

**Saeed Ghafouri** [1], **Mohammad Ali Hajiahmadi** [1], **Mehdi Firouzi** [2,*], **Gevork B. Gharehpetian** [1] ,
**Saleh Mobayen** [3,4,*] **and Paweł Skruch** [5]

1    Electrical Engineering Department, Amirkabir University of Technology, Tehran 15916-34311, Iran
2    Department of Electrical Engineering, Abhar Branch, Islamic Azad University, Abhar 45619-34367, Iran
3    Department of Electrical Engineering, University of Zanjan, Zanjan 45371-38791, Iran
4    Future Technology Research Center, National Yunlin University of Science and Technology,
     123 University Road, Section 3, Douliou, Yunlin 64002, Taiwan
5    Department of Automatic Control and Robotics, AGH University of Science and Technology,
     30-059 Kraków, Poland
*    Correspondence: mehdi.firouzi@iau.ac.ir (M.F.); mobayens@yuntech.edu.tw (S.M.)

**Abstract:** In this paper, the Unified Interphase Power Controller (UIPC) is utilized to protect the synchronous generator in case of faults occurring in the transmission system. The UIPC not only maintains the generator's stability by keeping its load angle within safe operational limits but also prevents high-amplitude currents from flowing through the stator windings. This also allows for more loading on the generator without compromising the system's stability. Moreover, utilization of the UIPC improves the LVRT capability of the generator by injecting reactive power at the faulted location. Additionally, a novel unified control scheme is proposed for the UIPC that enhances its performance by omitting the necessity of fault detection algorithms. To evaluate the performance of the proposed controller and the efficacy of the UIPC in protecting the synchronous generator under the faults, simulations have been conducted in a MATLAB/Simulink environment. A test grid was developed comprising a synchronous generator, transmission line model, UIPC, and an infinite grid representing the Point of Common Coupling (PCC), and three fault scenarios have been implemented in the transmission system. The comparative analysis of simulation results demonstrates the capability and efficacy of UIPC in isolating the synchronous generator from the faulted location, which in turn not only enhances transient stability of the generator, but also protects generator windings from detrimental faults currents. Moreover, according to the results, UIPC also contributes to recovering the voltage dip of the fault location via injecting reactive power.

**Keywords:** transient stability; synchronous generator; fault protection; UIPC; LVRT capability

## 1. Introduction

Power system stability is defined as its capability to retrieve its normal operating state (condition) after being exposed to any sort of transient or steady-state disturbance [1]. As demand for electricity increases continuously, the necessity of installing new power plants and establishing more and more interconnected systems with increased size and complexity emerges. This, in turn, invokes novel methods of system maintenance and protection for preserving synchronism among multiple system components. Short circuit faults are a major and significant source of disturbances, which can lead to the blackout of the entire system. Its destructive impacts on generators has been an incentive for the development of relay protection systems over the years. The protective relay configuration in these systems is accurately coordinated such that the overall system reliability is minimally affected due to short circuits or component failures [2].

However, as of now, electromechanical components such as circuit breakers comprise a major part of the control and protection systems. These mechanical components not only

have higher failure rates compared to static devices, but also the intrinsic time delay in the performance of such mechanical components and higher response times to control signals decreases the safe operation margin of the generation system, specifically synchronous generators (SGs) [3,4]. On the other hand, certain circuit breaker triggers may change the load on SGs considerably, which might result in its instability. These deficiencies impose many limitations on the operation of power systems.

In recent research studies, the flux control method has been proposed to overcome such latency in protection system performance in the case of connecting large-scale steam units to the power system [5]. However, since this method reduces the active output power of the generator, it can potentially lead to transient system instability due to the imbalance between generation and consumption. In recent decades, Flexible AC Transmission Systems (FACTS) have been used to enhance a system's transient and dynamic stability [6]. Utilizing FACTS devices enhances the safe operating margins of the generation and transmission systems, and thus the overall stability of the power system, mainly due to their low latency operation [4]. Therefore, in comparison with electromechanical breakers, preserving the same reliability using FACTS devices is less costly due to their higher operating margins and lower redundancies. STATCOM, SSSC, and UPFC are among the most commonly used FACTS devices in this field [6,7]. Additionally, several studies have been conducted on the optimal sizing and location of FACTS devices [8]. The STATCOM, which is installed in parallel with the transmission system, enhances the power quality via injecting a reactive current. SSSC is another FACTS device that is connected in series and regulates the local voltage profile. Neither of the aforementioned devices is capable of controlling the active and reactive power flow. On the other hand, UPFC which is connected in series and parallel with the transmission system can provide reactive power compensation via injecting the required reactive current into the installation bus. Nevertheless, the UPFC performance is constrained to a limited range [6].

The Unified Interphase Power Controller (UIPC) is a newly proposed member of the FACTS family which is connected in series with one transmission line. Its utilization in the power grid improves both steady-state operation of the system as well as recovery from transients that the system undergoes as a result of disturbances, such as sudden load changes or fault occurrences [9]. Under normal operation conditions, UIPC controls the flow of active and reactive power through the transmission system. On the other hand, the short circuit current limitation capability of UIPC enhances generator stability by stabilizing the load angle faster and thus preventing it from reaching the unstable zone during transient periods. This allows the generators' loading to increase and moves the system closer to its full generation capacity without compromising system reliability.

Several studies have already been conducted regarding applications of UIPC in power systems. In [8], the UIPC was introduced, modeled, and compared with IPC and UPFC. In [2], Alizadeh et al. analyzed distance relay performance in the presence of UIPC in the system. In [10], the performance of UIPC was investigated in controlling the wind farms' output power flow as well as their contribution to injecting current to the faulted location. The wind farm generators studied in this article are of the DFIG type. The authors of [11] utilized the UIPC to control the active and reactive power of wind farms to enhance the transient stability of the system. Here, the UIPC only protects the SCIG-based wind farm in case of faults occurring in the grid. A similar study [12] compares the efficacy of both UIPC and UPFC in enhancing the LVRT capability of a sample grid, including PV generation with the occurrence of faults. Here, since the UIPC is connected in series with the PV farm to control its power flow, thus, the transient stability of the SGs was not investigated. In [13], Zolfaghari et al. proposed an optimal UIPC control structure based on a fractional-order controller to enhance the bidirectional power flow control of the UIPC in hybrid microgrid clusters. The performance of the UIPC in this article is limited to normal operating conditions. In another study [14], the authors proposed a robust control scheme to compensate for the UIPC DC link nonlinear dynamics. The proposed method improves the accuracy of the power flow control capability of the UIPC in the

interconnected microgrids. Finally, the authors of [15] proposed a modified topology for the UIPC based on line power converters (LPCs) and a modified fuzzy logic controller. The major achievement in the aforementioned paper was to control the power flow in a grid-connected AC–DC microgrid.

In the present study, the UIPC is intended to maintain the stability of the synchronous generator by limiting the amplitude of oscillations of its load angle in case of fault occurrence. Additionally, during the faults, the UIPC absorbs the SG's active output power and converts it into reactive power, which is then injected into the faulted location, thus improving LVRT capability and the voltage profile of the faulted location. Moreover, a unified control scheme is proposed for the UIPC to enhance its performance without the need to detect the operating mode. The major contributions of this paper can be divided into two sections: First, a unified control scheme for both operating modes of the UIPC is proposed, and second, utilizing UIPC with the proposed control scheme to enhance generator transient stability is covered. The test system is simulated under a number of fault scenarios to assess the extent of performance improvement in terms of generator transient stability by UIPC. Simulations have been carried out in a MATLAB/Simulink environment. The results obtained from simulations demonstrate that by utilizing UIPC in the system, the load angle of the SG ($\delta$) is stabilized more rapidly to its final value, compared to the base system. This leads to higher system reliability in case of fault occurrences. As the results indicate, the stator current and voltage waveforms signify that, using UIPC, generator windings will suffer from fault currents with lower magnitudes and shorter durations, which protects them from the detrimental effects of high magnitude fault currents. Additionally, UIPC can mitigate the severe voltage drop at the fault location via injecting a reactive current.

The rest of this paper is organized as follows. In Section 2, the UIPC operation and its performance details are further introduced. In Section 3, a review of power system stability, the topology of the system under study, and the test scenarios, as well as the proposed UIPC control scheme, are explained along with the formulations. Simulation results and the respective discussions are included in Section 4. Finally, Section 5 concludes the paper.

## 2. UIPC Operation

UIPC is an interphase power controller (IPC) in which the phase-shifting transformers (PSTs) are replaced by voltage-sourced converters (VSCs) [9]. Its major superiority over IPC refers to the fact that VSCs do not have the phase-shifting limitations which are imposed on PSTs, as mentioned in [11,16,17]. Moreover, since the capacity of UIPC VSCs is merely dedicated to generating and transmitting required reactive power, the rating of the UIPC components is lower than that of other FACTS devices. The structure of the UIPC is illustrated in Figure 1.

Each phase of the UIPC is composed of three voltage source converters (VSCs), one in shunt and two in series connection with the system. The VSCs' connection to the high voltage transmission grid has been made possible through step-up transformers. The two series converters (SECs) are intended to regulate the UIPC bus voltage by adjusting the magnitude ($|V_{inj,i}|$) and phase angle ($\varphi_i$) of the injection voltages in each of the two series branches. Additionally, the purpose of the shunt converter (SHC) placement is not only to control DC capacitor voltage but also to adjust the voltage magnitude of the sending bus (see Figure 1). Therefore, both active and reactive power at the sending side of the network could be separately controlled. Active power is transmitted through the DC link and via VSCs, and, on the other hand, reactive power is autonomously generated or consumed via each VSC.

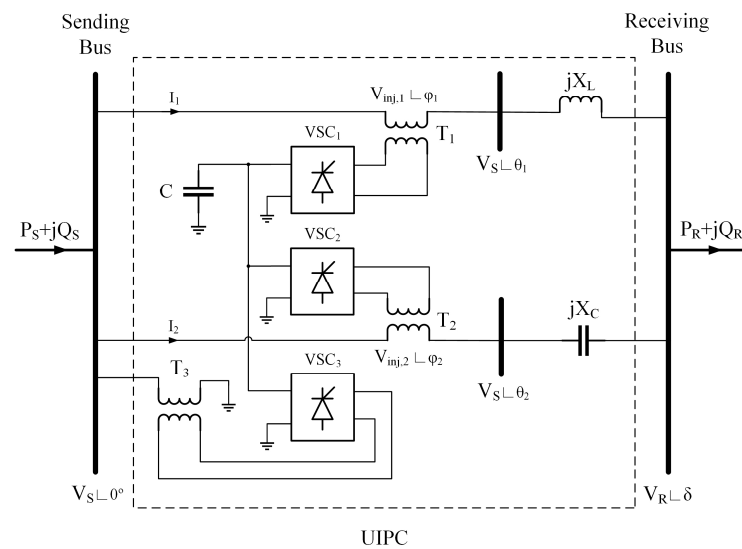In the following, both operating modes of the UIPC are briefly examined:

**Figure 1.** Single line configuration diagram for each phase of UIPC.

*2.1. Normal Condition*

As mentioned earlier, the main purpose of the UIPC placement in the power system is to control active power flow from the sending side—such as a microgrid—to another side and also to maintain acceptable voltage regulation. Active and reactive power delivered to the receiving bus ($P_R$, $Q_R$) are directly dependent upon UIPC current ($I_{UIPC}$). According to [11], using the source transformation theorem, this current can be formulated as Equation (1):

$$I_{UIPC} = I_1 + I_2 = \frac{V_S - V_S \angle \theta_1}{jX_L} + \frac{V_S - V_S \angle \theta_2}{-jX_C} \tag{1}$$

where, considering Figure 1, $I_1$ and $I_2$ are series branch currents, and vs. is the amplitude of the sending bus voltage. Under normal operating mode, since the voltages are sinusoidal and constant in magnitude, using the above equation, $P_R$ and $Q_R$ can be derived as follows [11]:

$$P_R = 2 \frac{|V_R||V_S|}{X} \sin(\alpha) \cos(\delta + \beta) \tag{2}$$

$$Q_R = 2 \frac{|V_R||V_S|}{X} \sin(\alpha) \sin(\delta + \beta) \tag{3}$$

where $X = X_C = X_L$ and both inductor and capacitor are tuned at system fundamental frequency. Moreover, $\alpha = (\varphi_2 - \varphi_1)/2$ and $\beta = (\varphi_1 + \varphi_2)/2$ are variables upon which $P_R$ and $Q_R$ are dependent, and $\delta$ is the phase angle of receiving bus voltage. Using (2) and (3), the following can be derived [11]:

$$|S_R| = \sqrt{P_R^2 + Q_R^2} = 2 \frac{|V_R||V_S|}{X} \sin(\alpha) \tag{4}$$

From (2) to (4), it can be deduced that using control variables $\alpha$ and $\beta$, the active and reactive power flowing through UIPC can be controlled. Additionally, since, under normal operating mode, $|V_S|$ and $|V_R|$ are constant, and for small values of $\alpha$, $\sin(\alpha)$ can be estimated with $\alpha$, apparent power ($S_R$) is a linear function of $\alpha$, and, thus, a PI controller can be used to calculate $\alpha$. Further details are explained in Section 3.3.

*2.2. Fault Condition*

The UIPC current can be decomposed into two orthogonal components $I_{UIPC}^P$ and $I_{UIPC}^Q$. The former corresponds with the active power flow, and the latter is responsible

for reactive power flow through the UIPC. These current components are formulated as Equations (5) and (6), respectively [10]:

$$I^P_{UIPC} = \frac{V_S}{X} \sin(\alpha)\cos(\beta)$$

(5)

$$I^Q_{UIPC} = \frac{V_S}{X} \sin(\alpha)\sin(\beta)$$

(6)

Based on the above equations, the amplitude and phase angle of the UIPC current are controlled by $\alpha$ and $\beta$, respectively. According to the grid code, not only must SGs remain in connection with the system under fault conditions, but they should also inject reactive current to compensate for the voltage drop [18]. The Low-Voltage Ride Through (LVRT) capability of the UIPC is feasible by controlling these variables, from which UIPC can contribute to voltage restoration of the faulted area by injecting reactive current. As soon as the fault is detected in the system, the UIPC's operating mode is switched. It is worth mentioning that the maximum feasible value for $\alpha$ corresponds with the SEC current rating of UIPC, which limits the amount of active and reactive power passing through the UIPC [10].

## 3. UIPC Control Scheme

### 3.1. Power System Stability

Under the steady-state operation of the SG, the input mechanical power derived to the rotor ($P_m$) is equal to the power drawn from the stator in electrical form ($P_e$) [19]. However, in the case of a sudden load change or occurrence of a fault, the transient power inequality causes the rotor speed to increase or decrease gradually, hence leading to a change in load angle ($\delta$) before the governor readjusts the $P_m$ [20]. According to what was mentioned, rapid fault clearance is of great importance in the power system. Critical Clearing Time (CCT) is the maximum permissible duration of a fault in terms of transient stability [21,22]. If the fault is cleared before CCT, the system remains stable; otherwise, it loses synchronism and, thus, becomes unstable.

In grids with a low R/X ratio, such as transmission systems, the active power flow between two nodes of the system can be described with Equation (7), in which $X_{eq}$ denotes the equivalent reactance in between, and $V_R$ and vs. are the voltage amplitudes at the two ends, with the phase angles of $\delta_S$ and $\delta_R$, respectively [23]:

$$P = \frac{V_S V_R}{X_{eq}} \sin(\delta_S - \delta_R)$$

(7)

Due to the phase-shifting capability of the UIPC, integrating it with the transmission system will modify the power flow equation with the control variable $\alpha$, as represented in Equation (8):

$$P = \frac{V_S V_R}{X_{eq}} \sin(\delta_S - \delta_R + \alpha)$$

(8)

Graphical representation of Equations (7) and (8) is depicted in the power-angle diagram in Figure 2. As can be seen, UIPC placement into the transmission line has caused the power curve to be shifted towards greater angles. The extent of this intermediate phase shift is characterized by the injected voltage of the series VSCs in UIPC.

Figure 3 illustrates the equal-area criterion for a synchronous machine transient stability margin with and without the presence of the UIPC in the system. A simplifying assumption is considered in Figure 3, which is the zero active power transfer during the fault period. Moreover, it is assumed that the fault is cleared before $\delta$ reaches the static stability limit of 90°. The UIPC control scheme maintains the maximum swing of the load angle from reaching stability margin via proper voltage injection through VSCs and thus, preventing the generator instability.
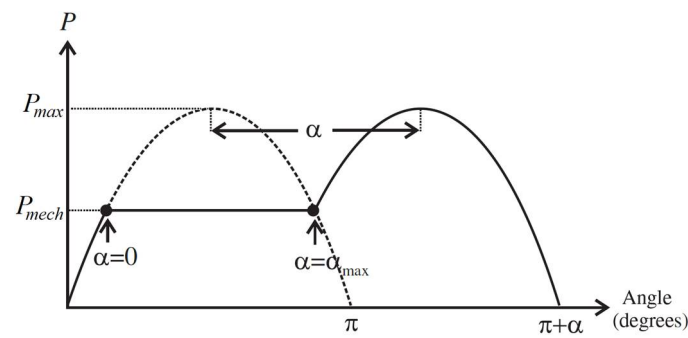
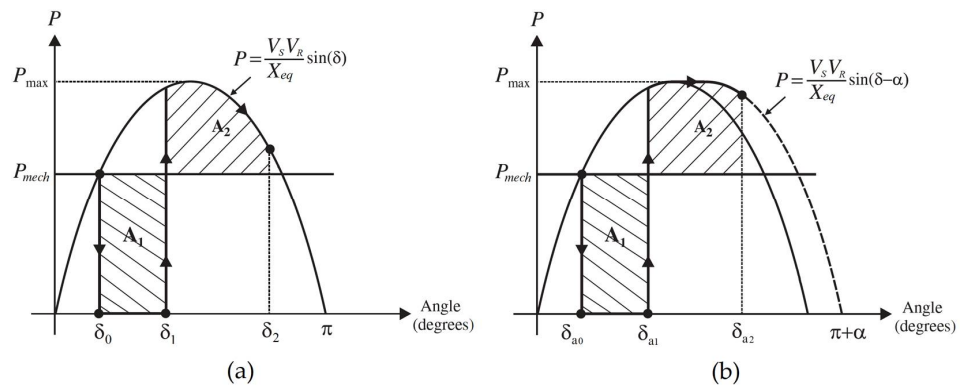**Figure 2.** Power angle diagram of the active power flow in a synchronous generator.



**Figure 3.** Equal-area criterion for transient stability of synchronous generator (**a**) without UIPC and (**b**) with UIPC.

### 3.2. System Configuration

To verify the performance of the proposed UIPC control scheme in enhancing generator stability, a sample test system is used. Figure 4 illustrates the configuration of the test system.
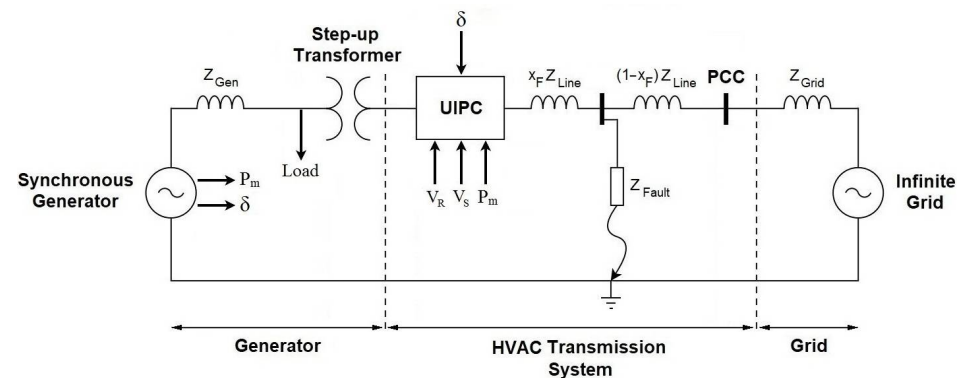


**Figure 4.** Schematic diagram of the test system with UIPC.

As depicted in this figure, the schematic diagram of the implemented test system consists of a synchronous generator and step-up transformer as its interface to the HVAC transmission system, UIPC, and an infinite bus, which represents the Point of Common Coupling (PCC) to the rest of the power grid. A fault is imposed on the system in the vicinity of the infinite bus (PCC) at t = 6 s and cleared at t = 6.3 s.

To fully assess the effectiveness of utilizing UIPC for enhancing the system's transient stability, three separate fault scenarios are defined as follows:

- Scenario 1: Three-phase to ground symmetrical fault;
- Scenario 2: Two-phase asymmetrical fault;
- Scenario 3: Three-phase fault with ground impedance.

The considerations behind the selection of these scenarios refer to the fact that, although three-phase-to-ground faults are rare in real conditions, they severely damage the equipment in the power system. Additionally, in the case of asymmetrical faults, normally, the voltage or current of other phases which are not imposed on the fault vary to great extents, and this has the potential of becoming crucial in SG transients. Finally, since faults with ground impedance occur more frequently than hard faults with zero impedance due to environmental conditions such as transmission lines falling on trees, etc. [24], it is investigated as a scenario in this paper. All the aforementioned fault scenarios have been implemented and simulated in MATLAB/Simulink environment [25].

### 3.3. The Proposed Control Strategy

During the fault condition, infinite bus voltage drops significantly below its rated value. Under these circumstances, voltage recovery can be achieved via injecting reactive current into the fault location [26]. The UIPC provides the required reactive current to mitigate this voltage drop. The DC link capacitor is charged through SHC via absorbing active power from the generator. By calculating firing angles $\psi_1$ and $\psi_2$ (see Figure 5), the UIPC controls the VSC switching pattern such that the required reactive current is generated from the energy stored in the capacitor. Therefore, the UIPC hinders the active power flow from the SG into the fault location.
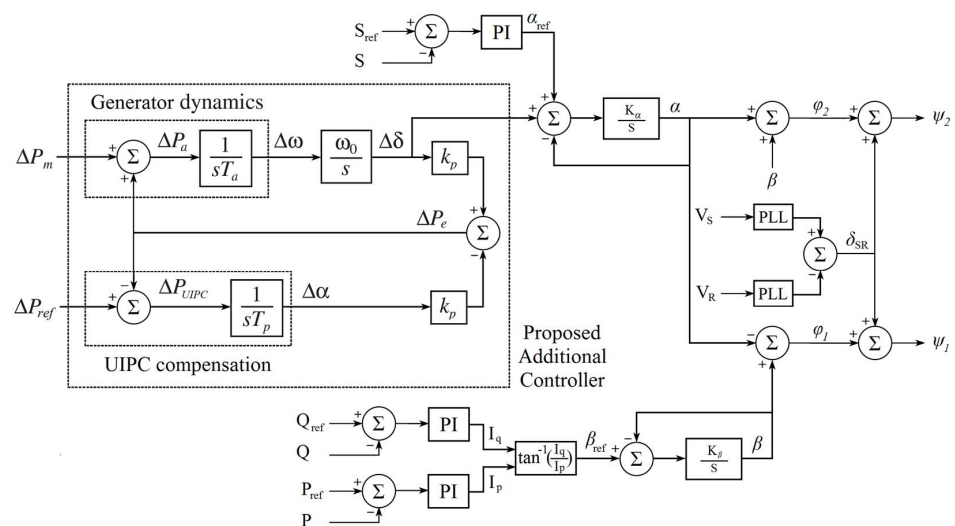


**Figure 5.** The proposed UIPC control scheme and series branches.

In [4,9–11], separate controlling schemes have been employed for normal and fault condition operating modes of the UIPC. The reason behind this refers to the fact that, under normal operation, the UIPC stabilizes the power flow to the receiving bus. Thus, by the occurrence of a fault in the receiving end, since the voltage drops significantly, the UIPC increases the injected current $I_{UIPC}$ to maintain the reference value for power flow. In other words, according to what was mentioned in Section 2 regarding the traditional control method, as soon as the fault is detected, the UIPC control approach is switched from the normal to fault condition to restrict the injected current to the fault location. However, in the proposed control scheme, an integrative controller is added to both $\alpha$ and $\beta$ calculation loops, which, according to Equations (5) and (6), results in a limitation over the UIPC injective current, preventing it from increasing unboundedly during the fault condition. The superiority of the proposed unified control scheme relies on bypassing the fault detection and operating mode alteration necessity during UIPC operation, as well as the decreased response time. Consequently, switching between different sets of controllers is omitted, thus providing a smooth transfer between operating modes.

The swing equation of the synchronous machine is as follows [27]:

$$
\begin{cases}
\frac{d\omega}{dt} = \frac{1}{T_a}(P_m - P_e) \\
\frac{d\delta}{dt} = \omega_0 \omega
\end{cases}
\tag{9}
$$

where $T_a$ denotes generator mechanical start-up time. Linearizing the above equation about the initial operating point yields Equation (10), as follows:

$$
\begin{cases}
\frac{d\Delta\omega}{dt} = \frac{1}{T_a}(\Delta P_m - \Delta P_e) = \frac{1}{T_a}\Delta P_a \\
\frac{d\Delta\delta}{dt} = \omega_0 \Delta\omega
\end{cases}
\tag{10}
$$

where $P_a$ is the change in accelerating power. On the other hand, the active power flow from the generator to the infinite bus is provided by Equation (11):

$$
P_g = \frac{E_g V_S}{X_{eq}}\sin(\delta - \alpha)
\tag{11}
$$

In the above equation, $X_{eq}$ denotes the reactance between the generator and the infinite bus, including the equivalent UIPC reactance and step-up transformer impedance. In the Laplace domain, the relation between the phase angle of the UIPC and the active power flow mismatch with respect to the reference value is as follows:

$$
\alpha = \frac{1}{sT_p}(P_{ref} - P_e)
\tag{12}
$$

where $T_p$ is the UIPC controller time constant. Due to the fast response of the Automatic Voltage Regulator (AVR) system of the machine, generator terminal voltage is kept constant, i.e., $E_g = 0$. Thus, linearizing Equations (11) and (12) about the actual operating point yields the following equation:

$$
\begin{cases}
\Delta P_e = k_p(\Delta\delta - \Delta\alpha) \\
\Delta\alpha = -\frac{1}{sT_p}\Delta P_e
\end{cases}
\tag{13}
$$

In the above equation, $k_p$ is calculated according to the initial conditions, that is:

$$
k_p = \left.\frac{\partial P_e}{\partial \delta}\right|_{\delta=\delta_0}
\tag{14}
$$

Based on Equations (10) and (14), the block diagram of the proposed control system for the UIPC is depicted in Figure 5. This figure demonstrates the diagram for the series branches of the proposed control scheme of the UIPC. As depicted in this figure, $\beta$ is calculated using the reactive to active current ratio, which in turn is comprised of active and reactive power control loops, while $\alpha$ calculation is based on the apparent power. Additionally, the control diagram of the UIPC shunt branch is depicted in Figure 6. As shown in this figure, the modulation index and firing angle of the SHC are calculated according to the voltage of the sending bus and DC link voltage, respectively.
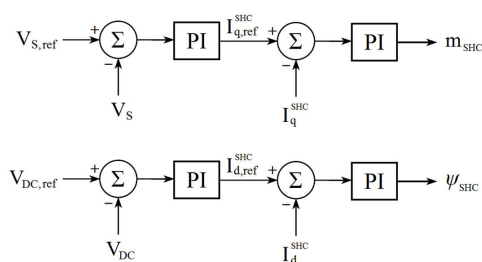


**Figure 6.** The proposed UIPC control scheme and shunt branch.

## 4. Results and Discussions

The simulation results from each fault scenario are presented and discussed in this section. Characteristics of the system components and UIPC parameters are gathered in Tables 1 and 2, respectively.

**Table 1.** Sample system components characteristics.

| Parameter | Value |
|---|---|
| System rated voltage | 230 kV |
| Generator rated power | 100 MW |
| Infinite grid rated power | 10 GW |
| Infinite grid impedance | 0.002 + j0.015 PU |
| Line length | 255 km |
| Line resistance per length | 0.025 Ω/km |
| Line inductance per length | 0.93 mH/km |
| Line capacitance per length | 0.013 F/km |
| Fault location ($X_F$) | 40% |

**Table 2.** UIPC parameters.

| Parameter | Value |
|---|---|
| Rated power | 100 MW |
| DC bus voltage | 40 kV |
| DC link capacitor | 2.5 mF |
| $X = X_L = X_C$ | 120 Ω |

### 4.1. Three-Phase-to-Ground Symmetrical Fault

In this scenario, a three-phase-to-ground (LLLG) is imposed on the system at the PCC bus. As depicted in Figure 7, the generator's load angle has significantly increased to the static stability margin (i.e., 90°) with the occurrence of the fault.
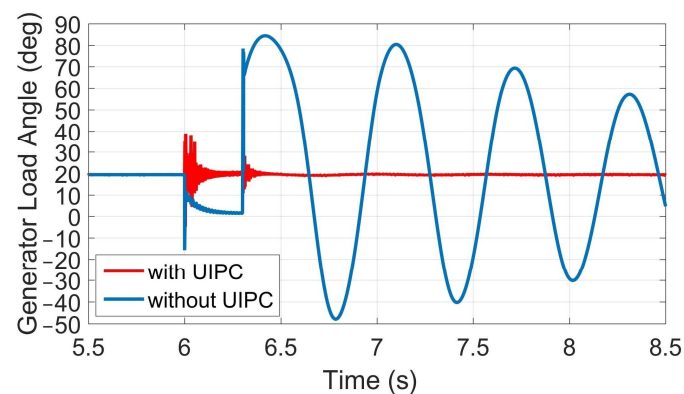


**Figure 7.** Generator load angle comparison, scenario 1.

However, according to this figure, in the system equipped with UIPC, the load angle has stepped up for much less than that of the base system, and the magnitude of oscillations is constrained to a few degrees, assuring the generator's transient stability. For a symmetrical fault condition, the profiles of voltage and current are the same for all three phases. Therefore, as shown in Figures 8 and 9, only the results for phase 'A' are investigated here.
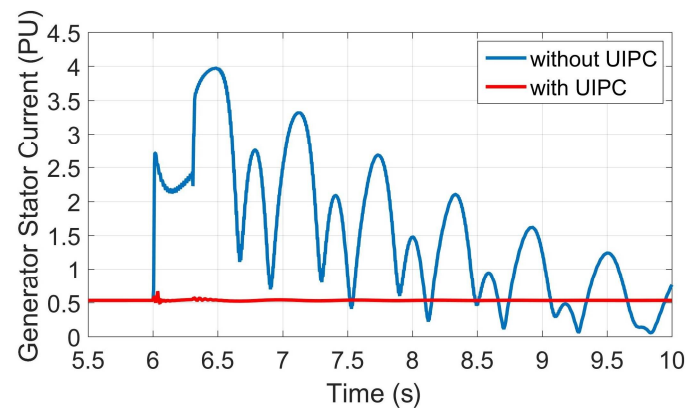
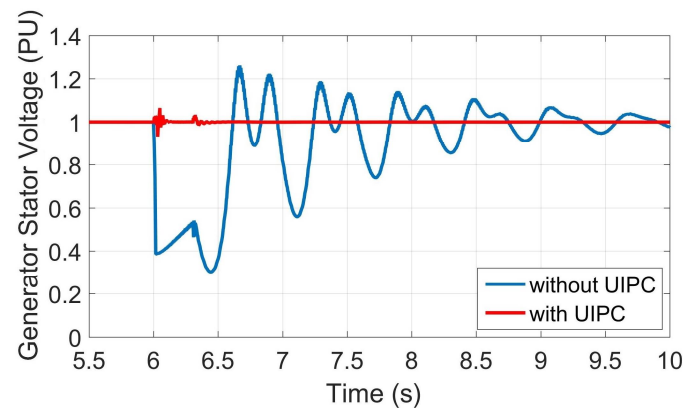**Figure 8.** Stator phase current comparison, scenario 1.



**Figure 9.** Stator phase-to-ground voltage comparison, scenario 1.

Figure 8 demonstrates the current flowing through generator windings as the fault is imposed and cleared from the system. According to this figure, in the base system, the magnitude of the peak current has reached up to 4 PU, and it also takes rather a long time to return to the 0.5 PU value before fault occurrence. This is while the amplitude of oscillations in the system equipped with UIPC is limited to 0.66 PU, and it is stabilized to the final steady-state value faster after fault clearance, preventing transient damage to generator windings.

Graphs of stator phase-to-ground voltage oscillations are shown in Figure 9. As can be seen from the point-to-point comparison between this and Figure 8, during the peak period of stator current, the voltage has reached its minimum value of 0.3 PU. The wide range of generator current fluctuations has led to the same for its voltage, ranging from 0.96 PU. Performance of the UIPC has constrained the amplitude of the variations to 0.13 PU which, compared to the base system, is a significant enhancement.

As mentioned earlier, UIPC isolates the generator side from the rest of the system. This is achieved by converting active power to reactive power using the stored energy in the DC capacitor (via altering VSCs' PWM switching pattern) at the time of fault occurrence. The amplitude and phase angle of the voltage over the UIPC series inductor are kept equal to those of the series capacitor during fault. Since $X_C = X_L$, the combination of two series branches creates a resonating circuit with infinite impedance, which isolates two sides of the UIPC. As depicted in Figure 10, the magnitude of reactive power consumed by the series inductor is equal to the reactive power generated by the series capacitor.
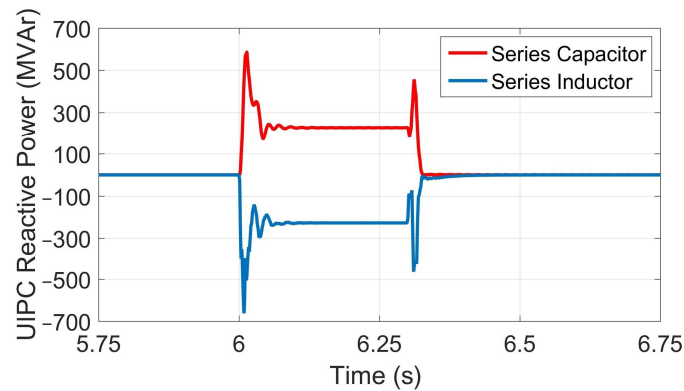
**Figure 10.** The UIPC reactive power balance during fault period, scenario 1.

### 4.2. Two-Phase Asymmetrical Fault

To analyze the efficacy of UIPC utilization under asymmetrical faults, an ungrounded phase-to-phase (LL) fault is implemented between phases A and B. Variations in generator parameters for all three phases are depicted in Figures 11–13, both with and without UIPC in the system.
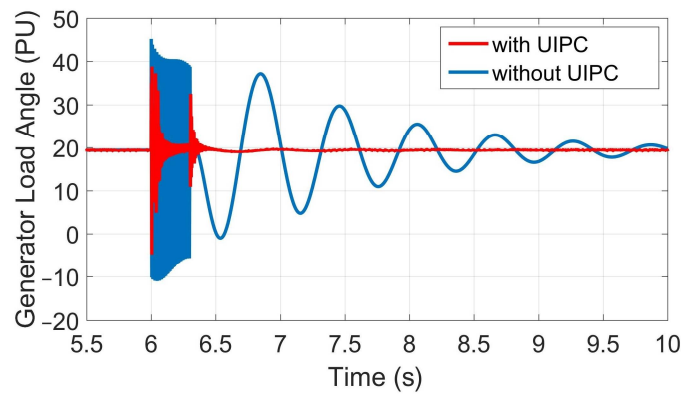


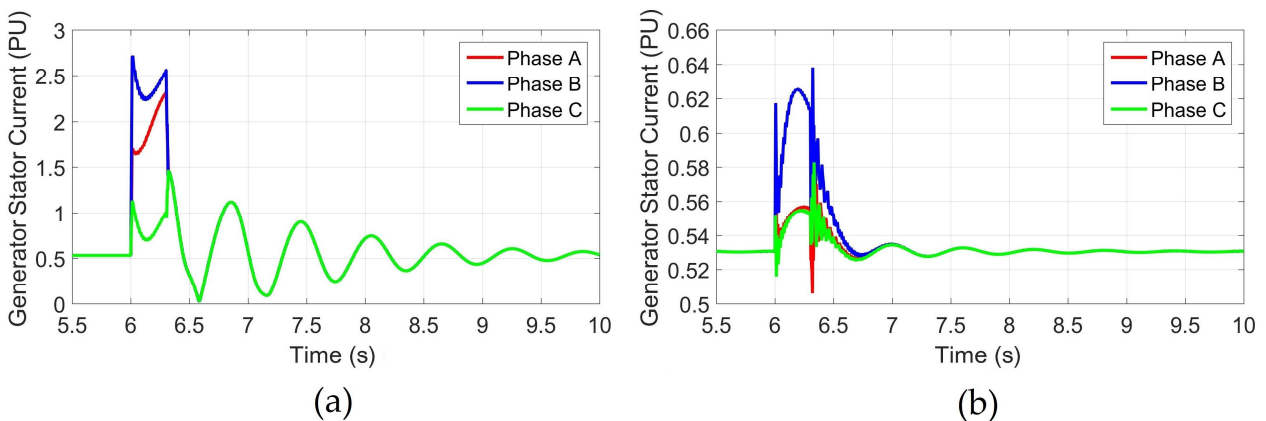**Figure 11.** Generator load angle comparison, scenario 2.



(a)

(b)

**Figure 12.** Stator phase current comparison (**a**) without UIPC and (**b**) with UIPC, scenario 2.
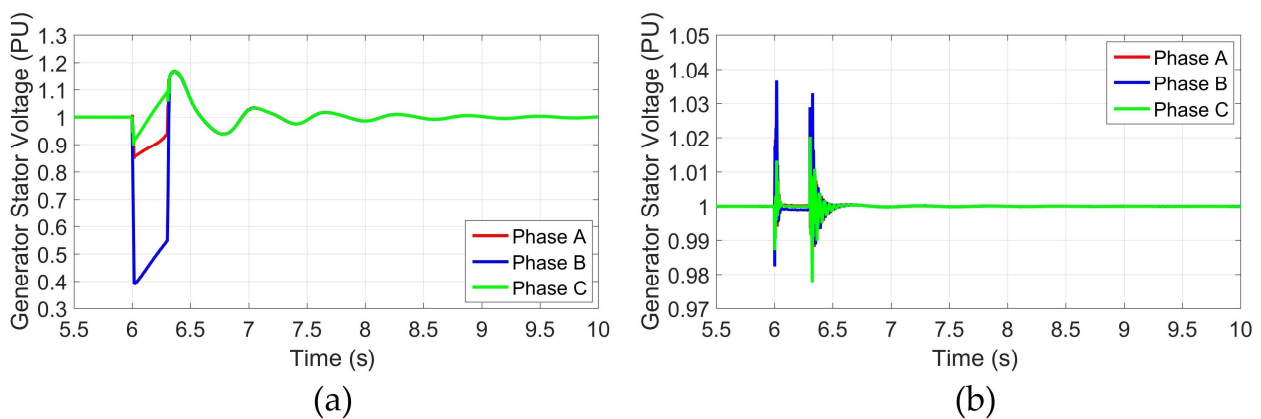
**Figure 13.** Stator phase-to-ground voltage comparison (**a**) without UIPC and (**b**) with UIPC, scenario 2.

As illustrated in Figure 11, load angle oscillations when utilizing UIPC in the system have stabilized much faster than in the base system. According to this figure, it can be concluded that although the amplitude of variations for both operation modes (with and without UIPC) does not differ significantly, the duration of large amplitude oscillations is shorter when UIPC is present in the system, i.e., the generator load angle is stabilized more quickly to the steady-state value of $\delta = 20°$.

In Figure 12, the stator current is illustrated for both operation modes. By comparing this with Figure 8, the peak current of phase B in the LL fault is lower than that of the LLLG fault, as expected.

Figure 13 demonstrates generator voltage oscillations. A comparison between Figure 13a with Figure 13b reveals that, in the base system, the stator voltage of phase B has declined to less than 0.4 PU, while the presence of the UIPC has mitigated the amplitude of voltage oscillations to less than 0.06 PU.

### 4.3. Three-Phase Fault with Ground Impedance

To investigate the performance of the proposed UIPC control scheme, a pure resistive ground impedance is implemented in the fault location. Based on Figure 14, it can be deduced that the presence of UIPC in the system has caused the voltage drop of the infinite bus to decrease significantly compared to the base system. This is due to the LVRT capability of the UIPC by injecting reactive power to the fault location during the transient period. In other words, in the case of fault occurrence, the UIPC passes through only the reactive current from the energy stored in the DC link capacitor.

Figure 15 depicts comparative load angle oscillations with and without UIPC in the system. As can be seen from this figure, UIPC has limited the range of load angle variations from 56° to 30°, with a shorter settling time compared to the base system. In Figure 16, the comparative values of stator current are illustrated for both operation modes. A comparison between this and Figure 8 demonstrates that the range of current oscillations for both operation modes in fault with ground impedance is significantly lower than that of zero impedance fault.

Graphs of stator voltage are shown in Figure 17. As depicted in this figure, by utilizing UIPC, voltage oscillations of the stator winding are limited to much lower values. Additionally, by comparing this with Figure 13, it can be seen that the amplitude of these oscillations includes a wider range under symmetrical fault without ground impedance in both operation modes (with and without UIPC utilization). This is because, with the occurrence of fault with ground impedance, the infinite bus voltage is higher, and the fault current passing through generator windings is of lower magnitude, resulting in lower phase-to-ground voltage over stator windings in transient periods.
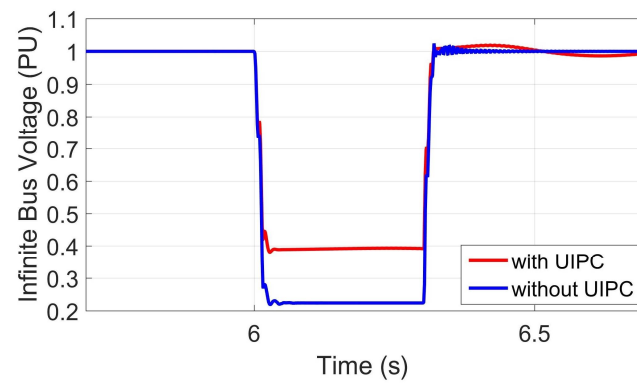
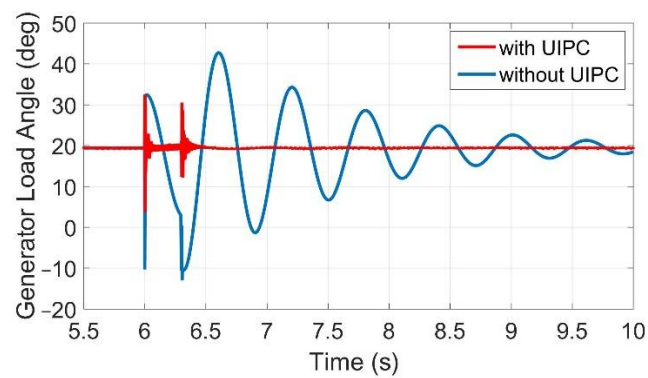**Figure 14.** Infinite bus voltage comparison, scenario 3.



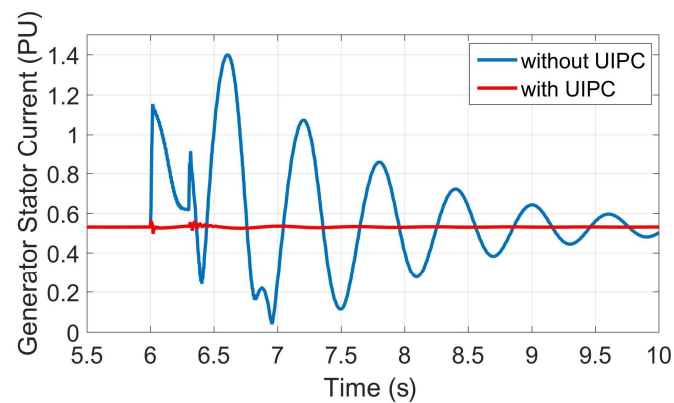**Figure 15.** Generator load angle comparison, scenario 3.



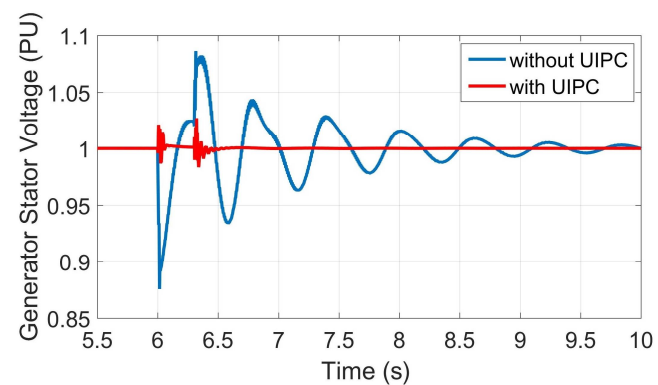**Figure 16.** Stator phase current comparison, scenario 3.



**Figure 17.** Stator phase voltage comparison, scenario 3.

Figure 18 illustrates the active power absorbed by UIPC in all three fault scenarios. As shown in this figure, it is only during the fault period that the DC link capacitor exchanges power with the system, and no active power is absorbed from or delivered to the system under normal operation when the PCC voltage is constant.
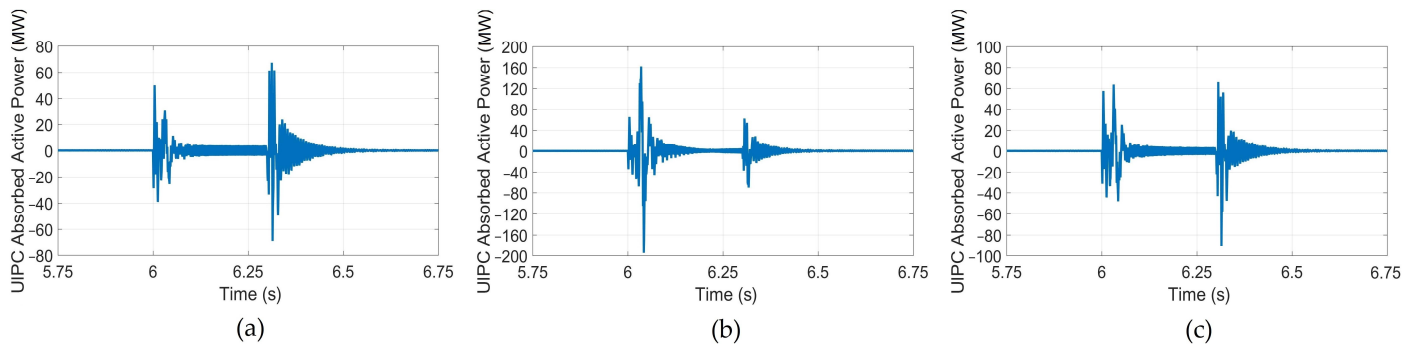


**Figure 18.** UIPC active power exchange with system: (**a**) scenario 1, (**b**) scenario 2, and (**c**) scenario 3.

## 5. Conclusions

In this paper, the effect of utilizing UIPC on improving a synchronous generator's transient stability as well as its LVRT capability under several fault scenarios in the transmission system is investigated. During the faults, the UIPC absorbs the generator's active power and generates reactive power through its VSCs, which is then injected into the faulted location to improve the voltage profile. This also limits the amplitude of oscillations of generator load angle within its safe operating range, preventing it from losing synchronism and becoming unstable. Furthermore, a new unified control scheme is proposed for the UIPC which obviates the need for mode transitions between normal operation and fault conditions, resulting in a smoother and, more importantly, faster response. The results obtained from system simulation under several fault scenarios reveal that the UIPC isolates the generator from the fault location, which not only stabilizes the generator load angle much faster, but its oscillation range is also effectively limited. This leads to a higher stability margin for the generator, thus enabling the system to be operated closer to its full installation capacity without compromising the system's stability. Additionally, in terms of generator protection, the application of UIPC in the system significantly decreases the short circuit current flowing in generator stator windings with a shorter duration, leading to less damage to the generator during the fault transients. Moreover, according to the results, the UIPC considerably enhances the voltage profile of the faulted location through reactive current injection.

## Nomenclature

| | |
|---|---|
| $P_R, Q_R, S_R$ | Active, reactive, and apparent power delivered to the receiving bus, respectively |
| $P_S, Q_S$ | Active and reactive power sent from the sending bus, respectively |
| $V_R, V_S$ | Voltage at the receiving and sending buses, respectively |
| $I_{UIPC}, I_{UIPC}^P, I_{UIPC}^Q$ | The UIPC current, its direct, and its quadrature component |
| $\left\|V_{inj,i}\right\|, \varphi_i$ | The magnitude and phase angle of each SEC injected voltage, respectively |
| $\delta$ | The phase angle of the receiving bus voltage, equal to the SG load angle |
| $P_m$ | Mechanical power delivered to SG rotor |
| $P_e$ | Electrical power drawn from SG stator |
| $E_a$ | The SG stator terminal voltage |
| $x_S$ | The SG stator reactance |
| $V_{DC}$ | The DC capacitor voltage |
| $\psi_1, \psi_2$ | The firing angles of the SECs |
| $m_{SHC}, \psi_{SHC}$ | The modulation index and firing angle of the SHC |
| $T_a$ | The SG mechanical startup time |
| $T_P$ | The UIPC controller time-constant |

## References

1. Milano, F.; Manjavacas, Á.O. Frequency-Dependent Model for Transient Stability Analysis. *IEEE Trans. Power Syst.* **2018**, *34*, 806–809. [CrossRef]
2. Alizadeh, M.; Khodabakhshi-Javinani, N.; Gharehpetian, G.; Askarian-Abyaneh, H. Performance analysis of distance relay in presence of unified interphase power controller and voltage-source converters. *IET Gen. Trans. Dist.* **2015**, *9*, 1642–1651. [CrossRef]
3. Eladany, M.M.; Eldesouky, A.A.; Sallam, A.A. Power system transient stability: An algorithm for assessment and enhancement based on catastrophe theory and FACTS devices. *IEEE Access* **2018**, *6*, 26424–26437. [CrossRef]
4. Firouzi, M.; Gharehpetian, G.B.; Mozafari, S.B. Application of UIPC to improve power system stability and LVRT capability of SCIG-based wind farms. *IET Gen. Trans. Dist.* **2017**, *11*, 2314–2322. [CrossRef]
5. Müller, T.; See, C.; Ghani, A.; Bati, A.; Thiemann, P. Direct flux control–sensorless control method of PMSM for all speeds–basics and constraints. *Electron. Lett.* **2017**, *53*, 1110–1111. [CrossRef]
6. Murali, D.; Rajaram, M.; Reka, N. Comparison of FACTS devices for power system stability enhancement. *Int. J. Comput. Appl.* **2010**, *8*, 30–35. [CrossRef]
7. Wibawa, B.C.; Prastiantono, A.; Aryani, D.R.; Setiabudy, R.; Husnayain, F. Transient stability improvement by FACTS devices: A Comparison between STATCOM and SSSC in an extra high voltage transmission system. *IOP Conf. Ser. Mater. Sci. Eng.* **2019**, *673*, 012068. [CrossRef]
8. Gaur, D.; Mathew, L. Optimal placement of FACTS devices using optimization techniques: A review. *IOP Conf. Ser. Mater. Sci. Eng.* **2018**, *331*, 012023. [CrossRef]
9. Pourhossein, J.; Gharehpetian, G.; Fathi, S. Unified interphase power controller (UIPC) modeling and its comparison with IPC and UPFC. *IEEE Trans. Power Deliv.* **2012**, *27*, 1956–1963. [CrossRef]
10. Firouzi, M.; Gharehpetian, G.B.; Mozafari, B. Power-flow control and short-circuit current limitation of wind farms using unified interphase power controller. *IEEE Trans. Power Deliv.* **2016**, *32*, 62–71. [CrossRef]
11. Firouzi, M.; Gharehpetian, G.B.; Salami, Y. Active and reactive power control of wind farm for enhancement transient stability of multi-machine power system using UIPC. *IET Renew. Power Gen.* **2017**, *11*, 1246–1252. [CrossRef]
12. Majlesi, A.; Miveh, M.R.; Ghadimi, A.A.; Kalam, A. Low Voltage Ride Through Controller for a Multi-Machine Power System Using a Unified Interphase Power Controller. *Electronics* **2021**, *10*, 585. [CrossRef]
13. Zolfaghari, M.; Abedi, M.; Gharehpetian, G.B. Power exchange control of clusters of multiple AC and DC microgrids interconnected by UIPC in hybrid microgrids. In Proceedings of the 2019 24th Electrical Power Distribution Conference (EPDC), Khoramabad, Iran, 19–20 June 2019; pp. 22–26.
14. Zolfaghari, M.; Gharehpetian, G.B.; Anvari-Moghaddam, A. Quasi-Luenberger observer-based robust DC link control of UIPC for flexible power exchange control in hybrid microgrids. *IEEE Syst. J.* **2020**, *15*, 2845–2854. [CrossRef]
15. Zolfaghari, M.; Abedi, M.; Gharehpetian, G.B. Power Flow Control of Interconnected AC-DC Microgrids in Grid-Connected Hybrid Microgrids Using Modified UIPC. *IEEE Trans. Smart Grid* **2019**, *10*, 6298–6307. [CrossRef]
16. Brochu, J.; Beauregard, F.; Lemay, J.; Morin, G.; Pelletier, P.; Thallam, R. Application of the interphase power controller technology for transmission line power flow control. *IEEE Trans. Power Deliv.* **1997**, *12*, 888–894. [CrossRef]
17. Zhang, Y.; Chen, C. A novel power injection model of IPFC for power flow analysis inclusive of practical constraints. *IEEE Trans. Power Syst.* **2006**, *21*, 1550–1556. [CrossRef]

18. Piwko, R.; Miller, N.; Girad, R.; MacDowell, J.; Clark, K.; Murdoch, A. Generator fault tolerance and grid codes. *IEEE Power Energy Mag.* **2010**, *8*, 18–26. [CrossRef]
19. Kothari, D.P.; Nagrath, I.J. *Electric Machines*; Tata McGraw-Hill Education: New York, NY, USA, 2004.
20. Khan, M.A.U.; Booth, C.D. Detailed analysis of the future distribution network protection issues. *J. Eng.* **2018**, *2018*, 1150–1154. [CrossRef]
21. Raju, R.G.G.; Subramaniam, N. Transient stability analysis employing equal area criterion. In Proceedings of the 2011 1st International Conference on Electrical Energy Systems, Chennai, India, 3–5 January 2011; pp. 275–280.
22. Sharma, S.; Pushpak, S.; Chinde, V.; Dobson, I. Sensitivity of transient stability critical clearing time. *IEEE Trans. Power Syst.* **2018**, *33*, 6476–6486. [CrossRef]
23. Eremia, M.; Shahidehpour, M. *Handbook of Electrical Power System Dynamics: Modeling, Stability, and Control*; John Wiley & Sons: Hoboken, NJ, USA, 2013; Volume 92.
24. Movahedi, A.; Niasar, A.H.; Gharehpetian, G.B. LVRT improvement and transient stability enhancement of power systems based on renewable energy resources using the coordination of SSSC and PSSs controllers. *IEEE Trans. Smart Grid* **2019**, *13*, 1849–1860. [CrossRef]
25. Blanquez, F.; Revuelta, P.; Rebollo, E.; Platero, C. Validation study of the use of MATLAB/Simulink synchronous-machine block for accurate power-plant stability studies. In Proceedings of the 2014 14th International Conference on Environment and Electrical Engineering, Krakow, Poland, 10–12 May 2014; pp. 122–126.
26. Taul, M.G.; Wang, X.; Davari, P.; Blaabjerg, F. An overview of assessment methods for synchronization stability of grid-connected converters under severe symmetrical grid faults. *IEEE Trans. Power Electron.* **2019**, *34*, 9655–9670. [CrossRef]
27. Marconato, R. Dynamic Behaviour, Stability and Emergency Controls. In *Electric Power System*; Italian Electrotechnical Committee (CEI) Standards: Rome, Italy, 2008; Volume 3.